The Application of Fraunhofer Diffraction Below 1µm to Particle Size Analysis from 0.1µm to 2000µm

S. Röthele, H. Naumann, Dr. M. Heuer

SYMPATEC GmbH, Clausthal-Zellerfeld, Federal Republic of Germany

---

Contents

---

* Extended version of the paper presented under the same title at PARTEC, Nürnberg, 1989

---

1 Introduction

During the interim, the application of the Fraunhofer method as a so-called laser diffraction technique has become so widespread that it may be regarded as the dominating standard among modern approaches. High speed and reproducibility of measurement, the wide domain spanned by each respective measuring range, as well as simplicity and convenience of operation are especially important benefits for the user.

Restrictions imposed by the principle on the measurement of small particle sizes below 5µm have resulted in the initiation of various developments. The purpose of these efforts is to overcome the lower limit of applicability, or at least to extend the range to values decidedly below 1µm, in part by a combination with other approaches, and in part by extension of the Fraunhofer method. Diffraction spectrometers designed for measuring down to about 0.1µm have become available on the market meanwhile.

The mutual interaction between light and small spheres is described by the Mie theory, whose limiting cases can be approximated in a simplified manner by Rayleigh scattering in the fine range and by Fraunhofer diffraction in the coarse range. Mie theory and Rayleigh scattering are characterized by a pronounced dependence on the optical constants of the system under investigation. However, these constants are usually unknown or, in the case of mixtures of substances, for instance, cannot even be determined unambiguously. Furthermore, the dependence on shape is still largely unknown, although this problem is only of subordinate importance in the Fraunhofer range.

The fundamental considerations which justify the application of the theory of Fraunhofer diffraction in the submicron range are explained. The manner in which reliable measurements can thus be performed - without the knowledge of material parameters such as the index of refraction and absorption coeffficient - is described. The capabilities of this technique, which is applied in

the SYMPATEC submicron HELOS instrument, are discussed on the basis of comparative results.

2 Fundamentals of diffraction spectrometry

Because of the references required in the following discussion, the fundamental principles of the instrument employed are first summarized. A detailed description is given in the publications of Heuer /1/ as well as by Heuer and Leschonski /2/.

As a rule, diffraction spectrometers are provided with an optical arrangement, such as that illustrated in figure 1. The diffraction

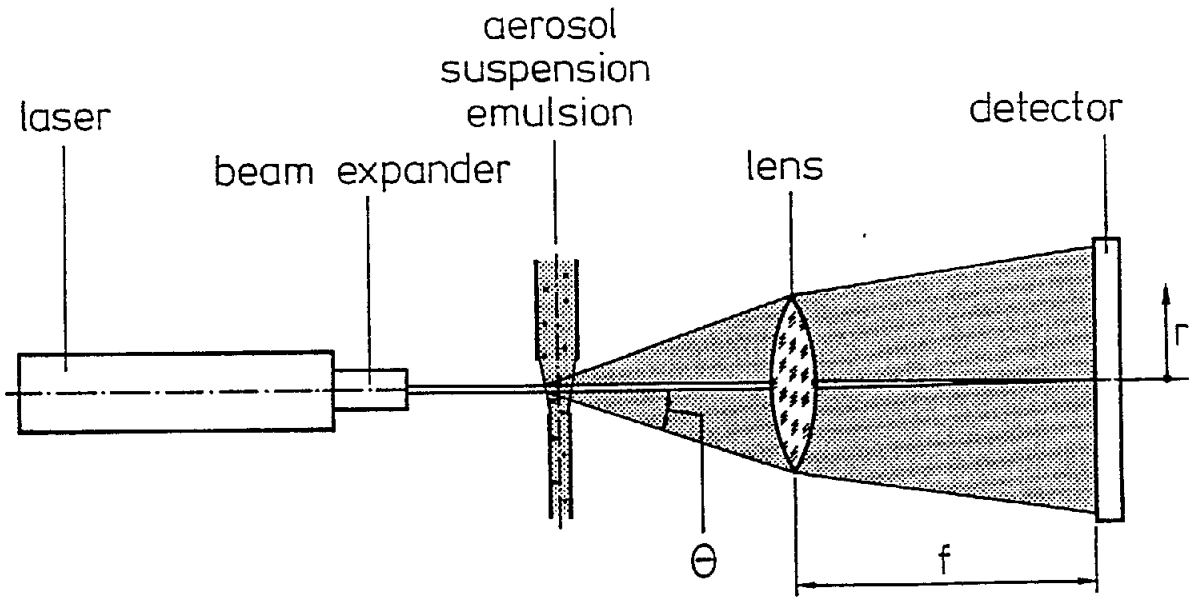

Figure 1: Optical arrangement for the generation of diffraction patterns

patterns are generated in the focal plane of the lens located downstream by the particles which are brought into the laser beam, and detected by a special sensor.

The evaluation is based on the Fredholm integral equation, which describes the intensity distribution, $I(r)$, of a particle collective by means of its density distribution by number, $q_0(x)$. The following equation applies in the focal plane of a lens, at a distance, r, from the focal point:

$$I(r) = \int_{X_{min}}^{X_{max}} N_{tot}\, q_0(x)\, I(r,x)\, dx \qquad (1)$$

$I(r,x)$ denotes the intensity distribution given by Airy for a sphere of diameter x:

$$I(r,x) = I_0\, (x^2\pi/2\, f)^2\, (J_1(z)/z)^2 \qquad (2)$$

with

$$z = (\pi r x/\lambda f) \qquad (3)$$

The Fredholm integral equation can be solved in closed form or numerically. The solution in closed form described by Shifrin /3/ and Chin /4/ utilizes the Mellin transformation indicated by Titchmarch /5/ and has been applied for the first time by Bayvel /6/. The solution thereby requires the differentiation of the measured values weighted with the third power of the angle; this task has still not been accomplished satisfactorily. Stable results calcultated by this method, especially in the limiting ranges of the particle size distributions, are not known to the authors.

All other methods of solution utilize numerical quadrature, that is, the transformation of the Fredholm intergral equation to a linear system of equations:

$$L = A\, q \qquad (4)$$

The luminous power, L, occurring at concentric annular detector elements situated in the focal plane of the lens is thereby computed. A is the matrix of coefficients which can be calculated from equation (2); its components represent the luminous power for inividual particles at the respective detector rings. q is the vector representing the desired spherical size distribution.

Systems of linear equations of this kind have the property of generating solutions of the following form, which oscillate strongly:

$$q = A^{-1} L \qquad (5)$$

Oscillations are thereby superimposed on the desired particle size distributions; these oscillations are much larger than the distributions themselves. Hence, the system of linear equations cannot be solved in a simple manner, as described by equation (5), since provision must also be made for suppressing the oscillations.

The simplest method of suppressing the oscillations is the advance specification of an analytical function for the particle size distribution with simultaneous minimization of the error squares. The approach was realized in a few initial instruments, and is in part still available as an option at present. However, the set of possible solutions is thus restricted to an extent which is not acceptable. For example, bimodal distributions are no longer recognizable in this case.

Among the numerous interative methods, those of Chahine /7/ and Mäkynen /8/, as well as that of Provencher /9/, have presumably been applied in two instruments. The smoothing and convergence properties of these techniques are very different, and their effect is difficult to appraise, since the type of measurements and of data acquisition are also decisive.

A parameter-free method is the smoothed solution described by Phillips /10/ and Twomey /11/; this approach utilizes the auxiliary condition that the density distribution is represented by a "Smooth" curve. Instead of equation (5), the following is obtained for the distribution density:

$$q = (A^T + \gamma H)^{-1} A^T L \qquad (6)$$

H denotes the smoothing matrix, which can be weighted with the Lagrange multiplier, γ. For a correct choice of γ, whose magnitude

depends on the optical construction and the quality of the data acquisition, among other factors, parameter-free particle size distributions can be measured by this method.

An overall survey of possible methods of solution is presented in table 1.

Fundalmental principle: Fraunhofer diffraction

Basis for evaluation : Fredholm integral equation

Solutions in principle: In closed form with the application of the Mellin transformation:

* Shifrin
* Chin
* Bayvel

Numerical Quadrature, that is, transformation to a system of linear equations

Methods of suppressing oscillations:

* Specification of an analytical function for the expected size distribution, for instance:
  - RRSB
  - ....
* Iterative methods:
  - Chahine - Mäkynen
  - Provencher
  - ....
* Smoothed solution (constrained inversion):
  - Phillips
  - Twomey

Table 1: Methods of solution for the analysis of diffraction patterns

3 Application to the submicron range

The measuring range for Fraunhofer diffraction extends from 1 to 3000µm and is thus very wide from the start. For a further extension to the region below 1µm (submicron range), however, the theoretical basis must first be examined. For spheres in this size range, the solution of Maxwell's equations in closed form, discovered by G. Mie in 1908, is applicable. This approach is now known as the Mie theory; it describes in a fundamental manner all interactions between light and a conductive sphere.

As illustrated in figure 2, the interactions are distinguished with the use of the terms reflection, diffraction, refraction, and absorption. The decisive component of diffraction is thereby described by the Fraunhofer solution.

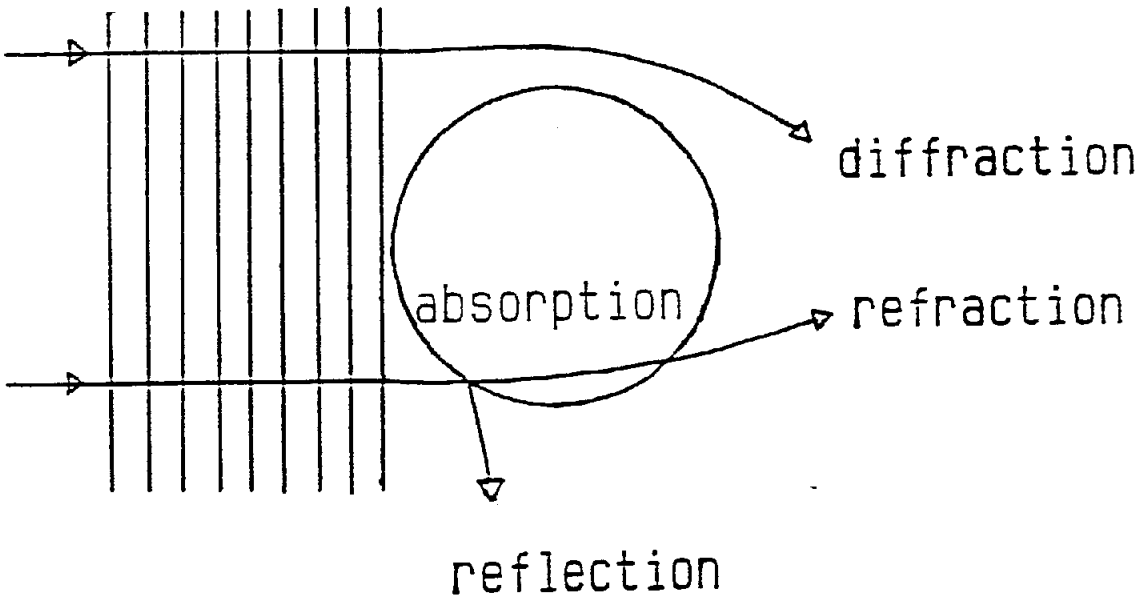

Figure 2: Interactions between light and a sphere /12/

The incident light is characterized by its wavelength, λ, and the radiation intensity, I_0. The interactive partner is defined as a sphere of diameter x, with the complex index of refraction, $m = n - ik$, where n is the refraction coefficient and k is the absorption coefficient. The intensity of the scattered light depends on these parameters in a manner governed by the scattering function,

$$i = f(\theta, x, \lambda, m), \qquad (7)$$

where θ represents the angle of observation (scattering angle).

The scattering behaviour is usually subdivided into three ranges, which are delimited by the Mie parameter:

$$\alpha = \pi \cdot x / \lambda \qquad (8)$$

The ranges are defined and compared in table 2.

Range		Scattering function	Proportionality
Rayleigh	$<< 1$	$i = f(\theta, \alpha, m)$	$i \approx x^6 / \lambda^4$
"Mie"	≈ 1	$i = f(\theta, \alpha, m)$	$(i \approx x^2)$
Fraunhofer	$>> 1$	$i = f(\theta, \alpha)$	$i(\theta \neq 0) \approx x^2$ $i(\theta = 0) \approx x^4$

Table 2: Scattering ranges

The designations "far greater than" and "far less than" indicate that the limits are not sharp, and that the transitions are gradual. These ranges, and the functions which are decisive there and indicated in table 2, are presented in figure 3.

For a scattering angle of 30 degrees, the scattering functions, in, are plotted against the Mie parameter in a double logarithmic diagramme. The curves designated by corresponding symbols exhibit the deviations calculated for the different specified values of the index of refraction, m. Besides the dependence presented in table 2 for the scattered light intensity on x^6 in the Rayleigh range and x^2 in the Fraunhofer range, the extremely pronounced influence of the index of refraction, m, is clearly evident. Differences in scattered light intensity by two orders of magnitude and more occur over wide ranges for a single particle size.

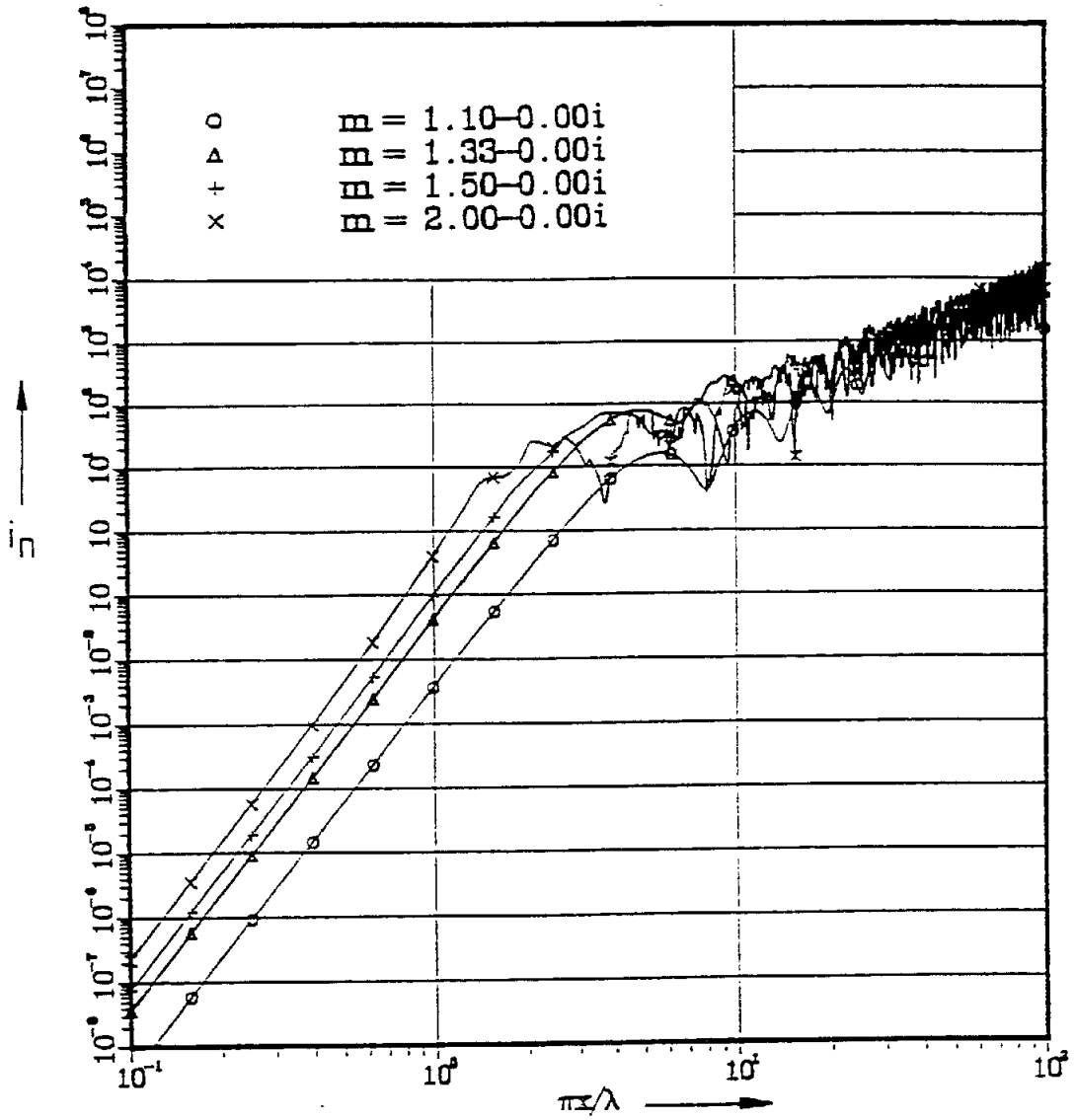

Figure 3: Scattering functions, i_n, for spheres with different refraction coefficients, n, calculated with the use of the Mie theory

The effect of the absorption coefficient, k, which has been varied in figure 4, is superimposed on this effect. In this case, recognizable variations are observed only for strong absorption in the Rayleigh range; outside of this range, variations occur even for slight absorption.

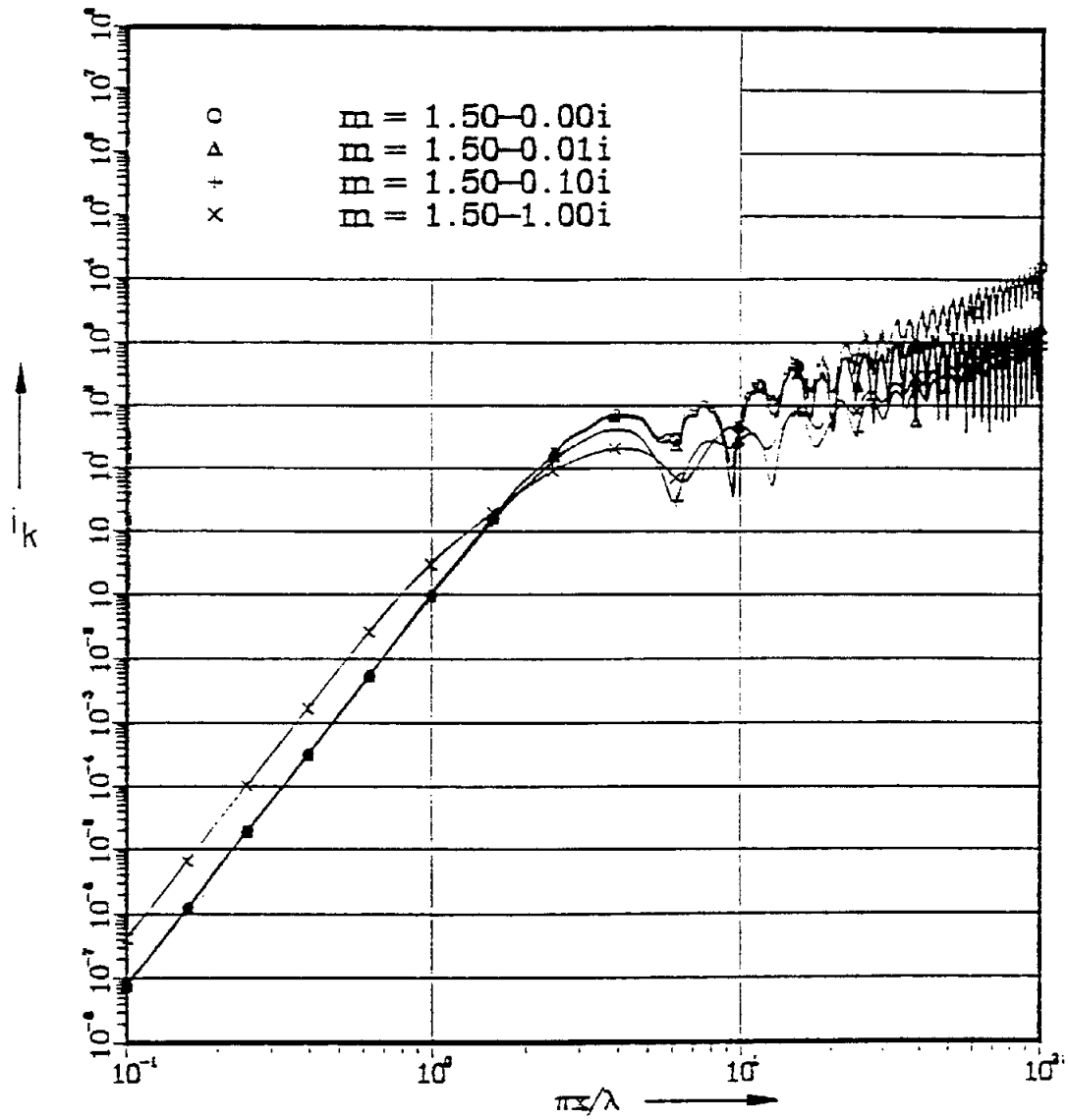

Figure 4: Scattering functions, i_k, for spheres of refraction coefficient, n, of 1.5, with different indices of absorption, k, calculated with the use of the Mie theory

The pronounced fluctuations in the so-called classical range for diffraction spectrometers, with x greater than 1µm, or α greater than 5, are clearly evident in figures 3 and 4.

For a correct application of the Mie equations to particle size analysis, therefore, knowledge of the complex index of refraction, m, is an absolute prerequisite. However, the refraction coefficient and absorption index, k are known only in exceptional cases. A solution is impossible for mixtures of different materials, for coated particles, and for processes in which the index of refraction varies. Furthermore, the reaction of the

system of equations to changes in shape of the sphere is uncertain. Moreover, the pronounced oscillations of the curves give rise to systems of equations which are even more unstable, and thus to matrices whose conditioning is less favourable; this, in turn, demands more drastic smoothing.

These effects of the index of refraction are difficult to overcome, and have therefore resulted in the following approaches: The limits on the "simple" and well proven Fraunhofer evaluation are examined, or an investigation is conducted to determine the particle size for which this dependence becomes effective, and to which extent, as well as the degree to which the gradual limits can be acceptably extended.

A preliminary consideration of the limiting case, $\alpha = 1$, yields the following results:

Medium	n_{liq}	λ nm	$x(\alpha=1)$/µm
Air	1	633	0,2
Water	1,33	476	0,151
Tetrachloroethene	1,504	421	0,134

Table 3: Particle sizes, **x**, for the limiting case, $\alpha = 1$

These results are based on the application of a He-Ne laser (with a value of 0.6328 µm for λ).

The application to liquids, which is the dominating application in the submicron range, requires the adaptation of the effective wavelength in accordance with

$$\lambda = \lambda_0 / n.$$

The resulting particle sizes, x, indicate that the limiting case under consideration, $\alpha = 1$, is not appreciably exceeded from below

with the inclusion of the submicron range for x greater than 0.1μm.

For appraising the expected deviations, the scattering function resulting from the application of the Fraunhofer solution in the range of $0,1 < \alpha < 100$ is considered and compared with that from the Mie curves.

The Fraunhofer scattering function, i_F, is plotted in figure 5.

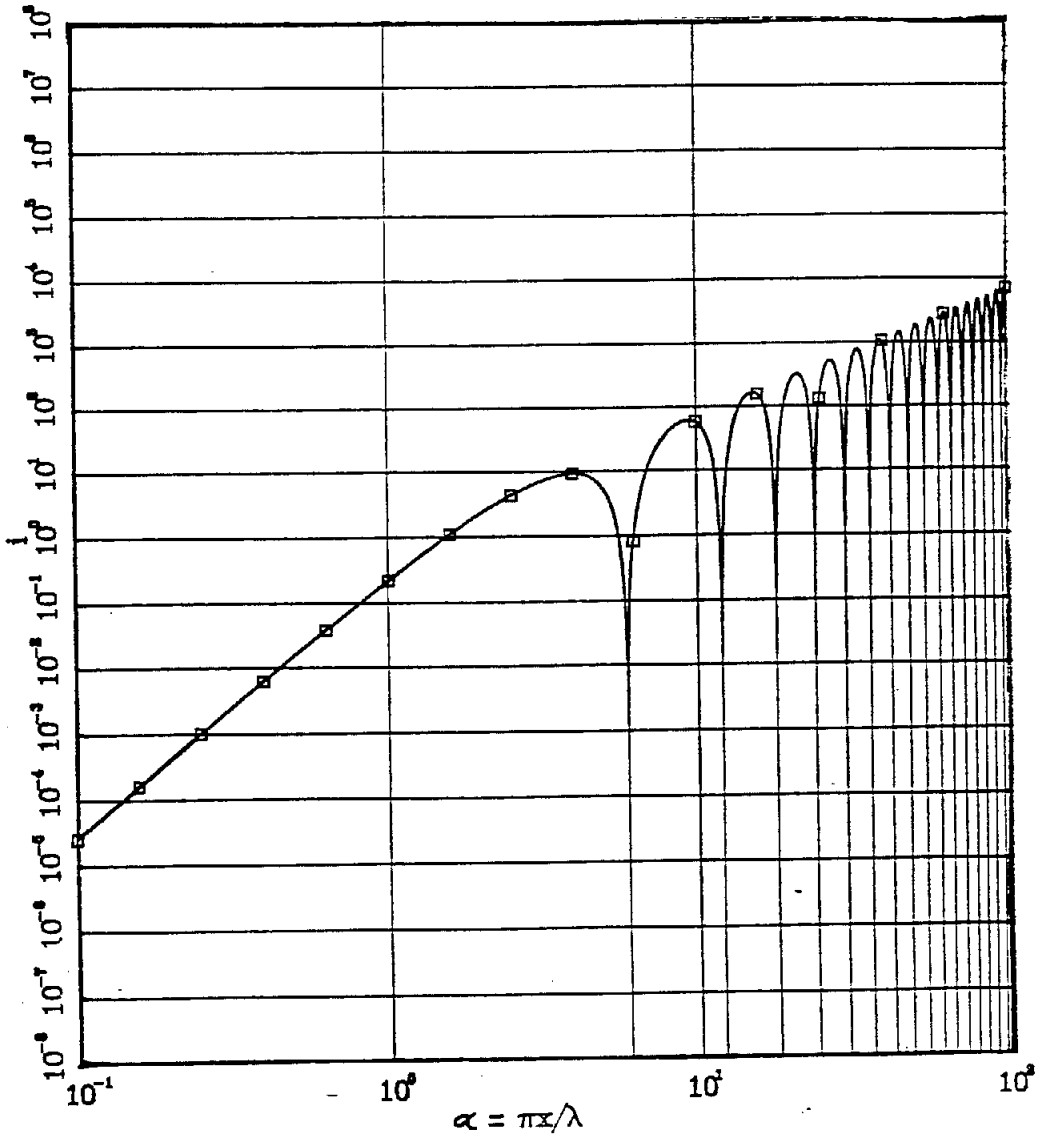

Figure 5: Scattering function, calculated from the Fraunhofer solution

With the application of the Fraunhofer solution, only one scattering function exists because of the independence of the index of refraction over the entire range of α. In the range of α between 0.1 and 1, it exhibits the expected increase in proportion with x^4 for small particles.

Within the range of α between 1 and 10, the first node of the Bessel function as well as the transition to the incipient increase in proportion with x^2 can be recognized; in the range of α from 10 to 100, this trend continues in the connection of the wave crests.

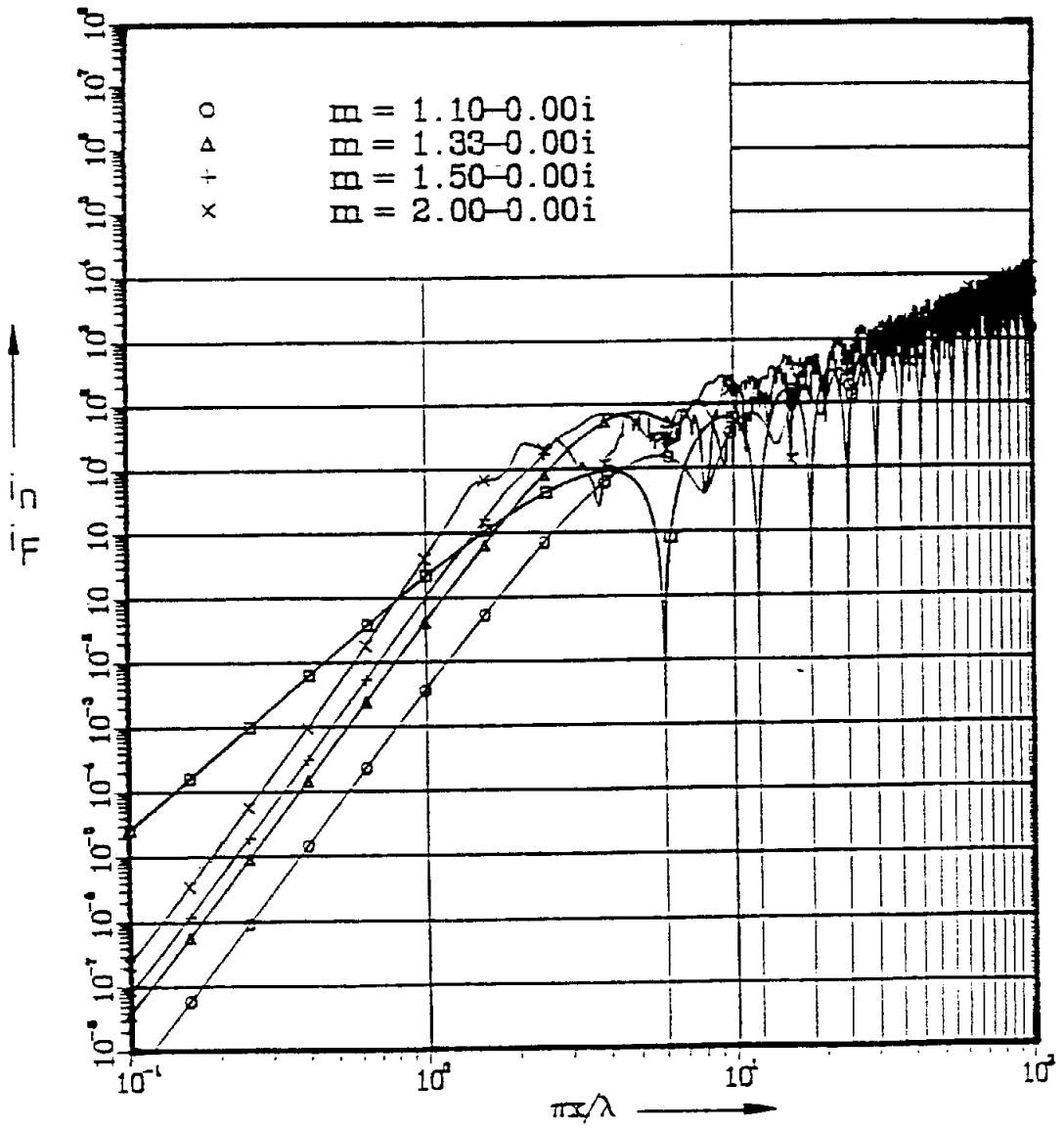

Figure 6: Comparison of the Fraunhofer scattering function with the Mie scattering functions of figure 3 (θ = 30°)

The nodes of the Bessel fuction (squares) is plotted in figure 6, in comparison with the scattering functions already presented in figure 3 for the Mie theory.

This direct comparison indicates that in the limiting range of α between 1 and 10, the Fraunhofer scattering function passes through the middle of the range which is spanned by the varied indices of refraction by means of the Mie solution.

From these considerations, it can be concluded that an incorrect assumption or restricted knowledge of the index of refraction can result in a greater uncertainty for the operator than resort to a method of evaluation hitherto regarded as not applicable in this range.

4 Selected results

Numerous systematic experiments have been conducted for testing the function of a Fraunhofer instrument modified in correspondence with this result in the range down to 0.1µm; several results of these tests are described in the present section.

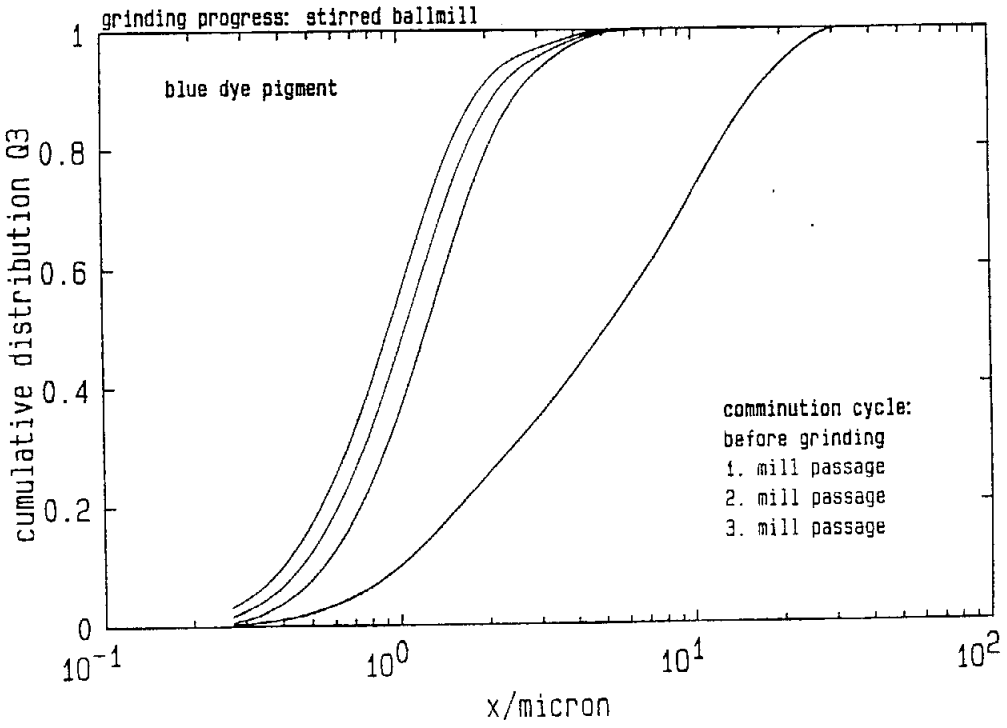

Figure 7: Measurements during grinding tests on a blue pigment

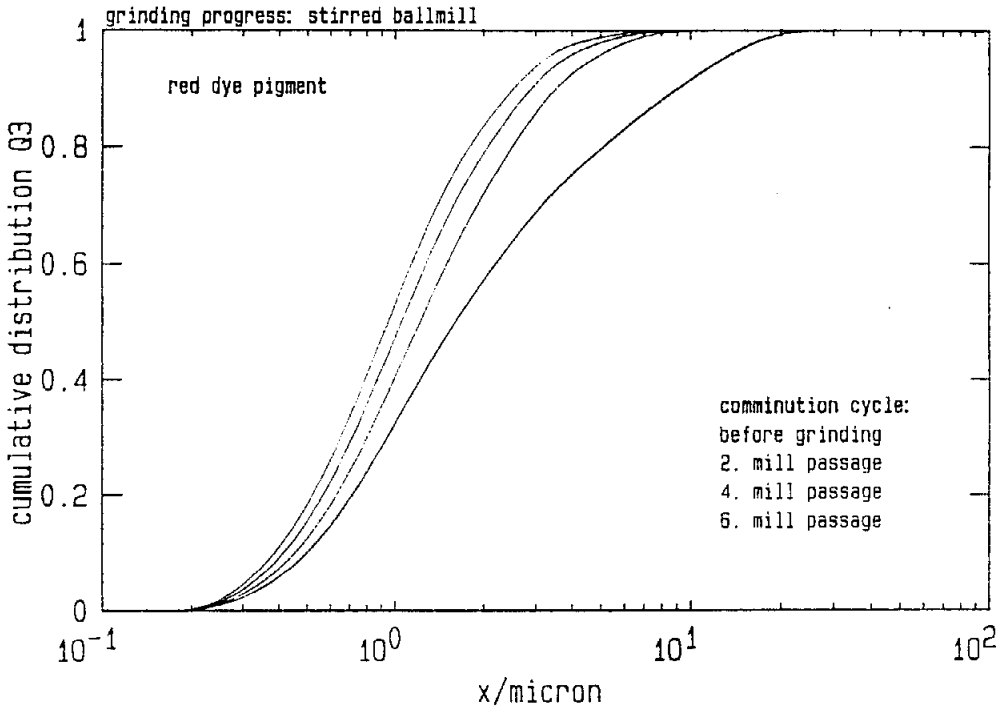

Figure 8: Measurements during grinding tests on a red pigment

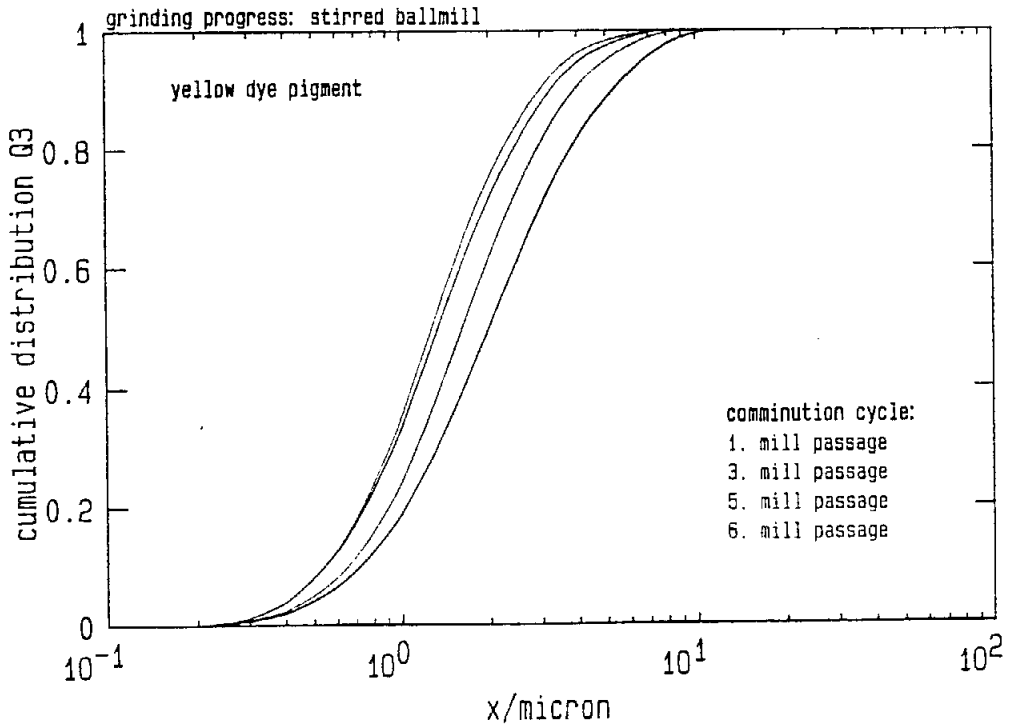

Figure 9: Measurements during grinding tests on a yellow pigment

The results of grinding tests on three different pigments are presented in figures 7, 8, and 9. The measurements were performed prior to grinding and after different numbers of grinding cycles (grcy) in stirred ball mills.

The "blue", "red", and "yellow" pigments exhibit both highly different indices of refraction and various shapes.

The blue particles had the shape of platelets, the yellow particles were rod-shaped, while the red particles did not exhibit any particular recognizable shape. Nevertheless, the grinding progress was demonstrated unambiguously and with a high degree of reproducibility. The progressive decrease in the efficiency with successive grinding cycles is likewise clearly evident.

These results demonstrate conclusively that variations in the particle size distributions in the submicron range are indicated reliably and reproducibly, at least in a qualitative manner.

Preliminary comparisons with other methods should provide a basis for reference. For gaining the closest possible access to "absolute" information for comparison, the present approach has been referred to scanning electron microscopy.

The cumulative distribution curves for specially prepared latex free of contaminants are plotted in figure 10.

The x_{50} values from the scanning electron micrographs (SEM) evaluated by Weichert /13/ by means of image analysis (IA) and those from diffraction analysis exhibit only a very slight mutual deviation, less than 0.02µm. The broadening of the distribution on the case of laser diffraction was expected, and occurs in the same form with the application of the Mie solution, since this effect results from the smoother curve shape of the scattering function in this size range.

A further comparison between SEM and HELOS is shown in figure 11 for a blue pigment.

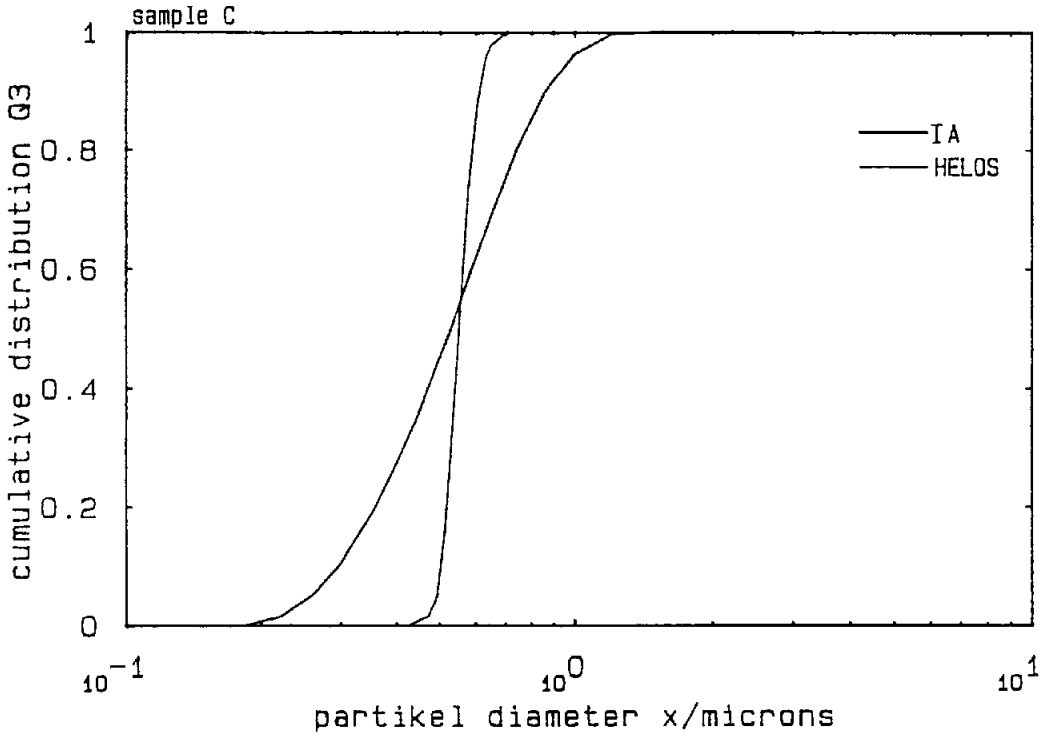

Figure 10: Cumulative distribution curves for latex with HELOS and image analysis (IA)

Besides the position, the shape, course, and width are very typically reproduced with this broad distribution. The width of the distribution is reproduced practically identically, whereas the x_{50} value is shifted by about 1.1µm toward coarser values.

A detailed, conclusive comment is not yet feasible without an in-depth consideration of scanning electron microscopy, especially in view of the very elaborate preparatory techniques associated therewith.

The extreme case of a distribution situated at the edge of the measuring range, measured with HELOS on a commercial drawing ink, is shown in figure 12. The distribution located at the lowermost edge of the measuring range cinfirms the sensitivity of the instrument even in that region. Precisely because eleven true measuring points are available below 1µm, and because the points are graduated, a particle size distribution is feasible even if all particle sizes are below 0.4µm, as in the preceding example, even if more than 50 per cent are situated below the measuring range covered.

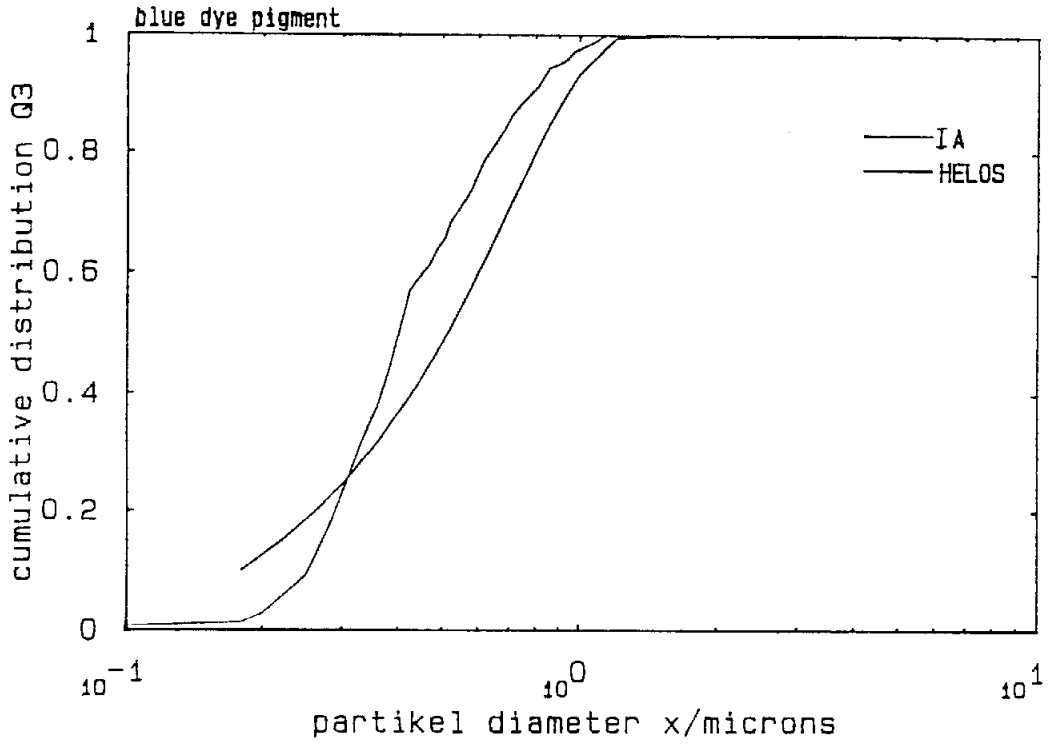

Figure 11: Cumulative distribution curves for a blue pigment, measured with HELOS and image analysis

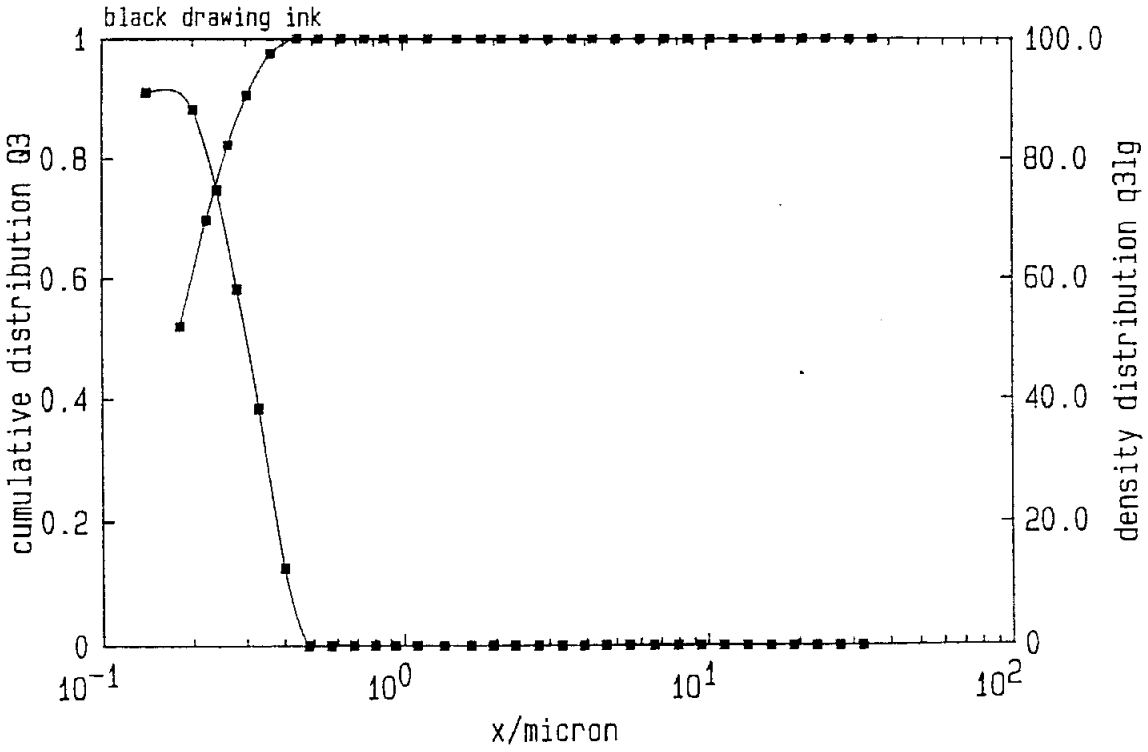

Figure 12: Cumulative distribution curve for a commercial drawing ink, measured with HELOS

5 Comparison of methods

Finally, a comparison with other submicron methods is presented. As a rule, these have been developed for use on particles smaller than 1µm, and the associated measuring range is usually restricted to the submicron region. Nevertheless, the comparison provides an impression of the results which can be achieved with these instruments.

The cumulative distribution curves measured on a blue pigment by various methods are plotted in figure 13; these curves supplement the results presented in figure 11 for HELOS and SEM.

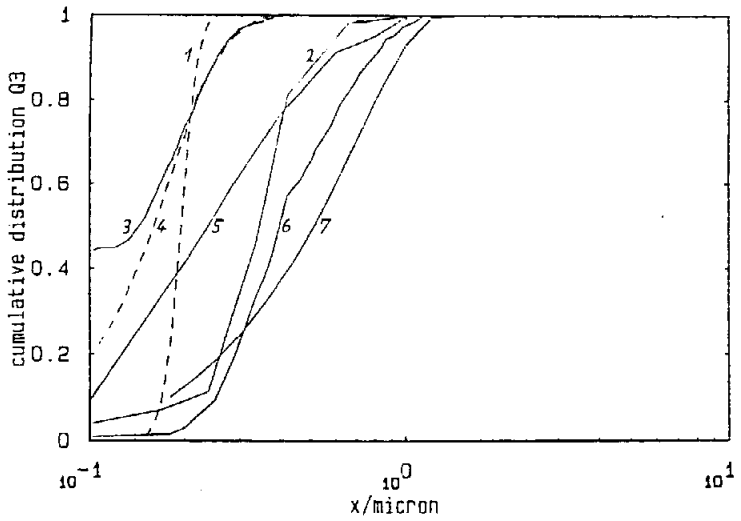

Figure 13: Results of measurements performed on a blue pigment (as in figure 11) by autocorrelation, polarization rotation, centrifuge, SEM, and HELOS

1. Autocorrelator
2. Polarization rotator, coupled with diffraction spectrometer
3. Experimental autocorrelator, evaluation model 1
4. Experimental autocorrelator, evaluation model 2
5. Commercial centrifuge
6. SEM with image analysis
7. HELOS

The results obtained with the autocorrelators are decidely shifted toward finer values; they do not reproduce the width of the distribution, and are apparently rotated systematically about the 0.2µm value in such a way that their width appears to allow selection. These large deviations are certainly due to several causes. The most serious reason is surely the fact that the

distribution for this blue pigment tends to be broader for an autocorrelator, and thus causes the intensity of the scattered light to vary over an excessively wide range. Moreover, the pronounced deviation of the particle shape from sphericity exerts an incalcuable influence. For autocorrelators, this distribution is situated at the upper limit of the measuring range, where a long measuring time is a prerequisite for stable results, for statistical reasons.

For a value of x_{max} which agrees rather well with the SEM result, the centrifuge yields a considerably finer distribution, whose deviation toward finer values steadily increases; consequently, the overall curve becomes very flat and broad.

The polarization rotator coupled with a diffraction spectral analyzer provides results near the SEM results in the fine range; in the upper range, however, the values are considerably finer and too steep on the whole.

In part, drastic deviations are observed with methods which theoretically should be capable of operating correctly in the range below 1µm; thus, the indicated deviations between SEM and HELOS appear all the more insignificant. These results verify the applicability of modified laser diffraction as a method of obtaining at least a good, and in many respects a reliable approach in the submicron range.

6 Conclusions

A brief survey of the fundamental physical principles and possible approaches is provided for the application of the Fraunhofer method to the analysis of particle size distributions with the use of so-called laser diffraction. Scattering functions for the Fraunhofer solution and the superimposed effects of refraction and absorption with the Mie method are compared; on the basis of these considerations the submicron range up to a value of unity for α is included in the successful Fraunhofer concept.

On the basis of experimental results, the applicability of the method is confirmed by a high degree of reproducibility and the reliable indication of both qualitative and quantitative size effects. Present knowledge and experience indicate that limitations and restrictions associated with the principles involved are no more serious than they are for other comparable techniques, or for methods hitherto regarded as more appropriate.

As a designer and manufacturer of measuring instruments, we also consider it our responsibility to provide the user with practical solutions for limiting ranges, too. The topic discussed involves the boundary conditions for the application of Fraunhofer diffraction in the submicron range. In our opinion, this also includes the logical and promising extension to information from measurements performed with the instrument in the limiting range with well known but reasonable restrictions on the conclusions concerned. We consider this approach better than to assure the user with apparently well proven methods and thus to impose unreasonable demands on his skills in everyday practice.

The necessary inclusion of parameters which ultimately cannot be reliably ascertained, such as the temperature-dependent refraction coefficient and absorption coefficient, thereby shifts the uncertainty of the measured result to inputs by the user and the external conditions in the area surrounding the instrument.

In view of the current status of ascertained knowledge, the user cannot by any means be absolutely sure of obtaining the "physical truth" about his product with the application of any measuring technique whatsoever, especially in the limiting ranges.

Nevertheless, laser diffraction with the use of the Fraunhofer method is in the process of reliably spanning the size range between 0.1 and 10000µm, and thus of further enhancing its dominating position among optical methods.

Appendix

7 References

/1/ M. Heuer: Verfahren zur Berechnung von Partikelgrößenverteilungen aus Beugungsspektren. 3. Fachtagung "Granulometrie 1983" 15.12.1983 Technische Hochschule Dresden.

/2/ M. Heuer, K. Leschonski: "Erfahrungen mit einem neuen Gerät zur Messung von Partikelgrößenverteilungen aus Beugungsspektren. Vortrag bei der PARTEC, 3. Europäisches Symposium "Partikelmeßtechnik" in Nürnberg, 9. - 11. Mai 1984.

/3/ K.S. Shifrin: (1956) Trudy VZLTI (Leningrad) No. 2 S. 153-162

/4/ J.H. Chin, C.M. Sliepcevich, M. Tribus: Determination of particle size distributions in polydispered systems J. Phys. Chem. 59 (1955), S. 845-848

/5/ E.C. Titchmarsh: Introduction to the Theory of Fourier Integrals, Oxford 1924

/6/ L.P. Bayvel, J.C. Knight, G.N. Robertson: Application of the Shifrin-inversion to the Malvern particle sizer. International "Symposium on optical particle sizing: Theory and practice", 12.-15. Mai 1987 INSA de Rouen.

/7/ M.T. Chahine: Determination of the Temperature Profile in an Atmosphere from its Outgoing Radiance. Journal of the Optical Society of America, Vol. 58, No. 12, Page 1634, 1968

/8/ J.M. Mäkynen: A Test of an Inversion Method for Determination of Particle Size Distribution from Light Scattering Pattern. The Eleventh Annual Conference of the Association for Aerosol Research: Aerosols in science, medicine and technology

/9/ S.W. Provencher: An eigenfunction expansion method for the analysis of exponential decay curves. The Journal of Chemical Physics, Vol. 64, No. 7, Page 2772ff., 1. April 1976

/10/ B.L. Phillips: A technique for the numerical solution of certain integral equations of the first kind. J.ACM, 9(1962)84

/11/ S. Twomey: "Introduction to the Mathematics of Inversion in remote sensing and indirect Measurements", Elsevier, Amsterdam, 1977

/12/ Normentwurf des Arbeitsausschusses optische Meßverfahren: Photometrische Meßverfahren

/13/ R. Weichert: "Partikelgrößenanalyse submikroskopisch kleiner Partikel in Suspension" (persönl. Mitteilung 1988; Veröffentlichung in Vorbereitung), Universität Karlsruhe, Institut für Mechanische Verfahrenstechnik und Mechanik

Nomenclature

A	Matrix of coefficients
f	Focal length
H	Smoothing matrix
i	Imaginary part
i_F	Scattering function for Fraunhofer solution
i_k	Scattering function, as a function of the index of absorption
i_n	Scattering function, as a function of the refraction coefficient
I	Luminous intensity
I_0	Intensity of laser beam
J_0	Bessel function of the first kind and zeroth order
J_1	Bessel function of the first kind and first order
k	Absorption coefficient
L	Luminous power
m	Index of refraction for the particle
n	Coefficient of refraction
n_{liq}	Coefficient of refraction for liquid
N_{tot}	Total number
q	Vector of the desired size distributions values
q_0	Density distribution by number
q_2	Surface density distribution
q_3	Volume density distribution
Q_3	Cumulative volume distribution
r	Radius of the focal plane
z	Abbreviation
α	Mie parameter
γ	Lagrange multiplier
θ	Scattering angle
λ	Wavelength
λ_0	Wavelength in vacuum